Applied Surface Science 267 (2013) 30–34

Contents lists available at SciVerse ScienceDirect

Applied Surface Science

journal homepage: www.elsevier.com/locate/apsusc

Hydrogen behaviour in amorphous Si/Ge nano-structures after annealing

C. Frigeri[a,*], M. Serényi[b], N.Q. Khánh[b], A. Csik[c], L. Nasi[a], Z. Erdélyi[d], D.L. Beke[d], H.-G. Boyen[e]

[a] CNR-IMEM Institute, Parco Area delle Scienze 37/A, 43100 Parma, Italy
[b] Research Institute for Technical Physics and Materials Science, Hungarian Academy of Sciences, P.O. Box 49, H-1525 Budapest, Hungary
[c] Institute of Nuclear Research of the Hungarian Academy of Sciences, P.O. Box 51, H-4001 Debrecen, Hungary
[d] Department of Solid State Physics, University of Debrecen, P.O. Box 2, H-4010 Debrecen, Hungary
[e] Institute for Materials Research, Hasselt University, Diepenbeek, Belgium

ARTICLE INFO

Article history:
Available online 11 May 2012

Keywords:
Amorphous Si/Ge superlattice
Hydrogen
Annealing
Nanostructure
Blistering

ABSTRACT

The relationship between blistering, H content and de-passivation of the dangling bonds has been studied in annealed hydrogenated a-Si/a-Ge superlattice (SL) nanostructures grown by RF sputtering. Measurements have been carried out by ERDA, IR absorbance and AFM. By comparison with parallel investigations on a-Si and a-Ge single layers it has been established that the bubbles causing blistering in the annealed SLs very likely start to grow in the Ge layers of the SL because H is released from Ge much earlier than from Si. It is shown that the H forming the bubbles is only a fraction of the H liberated during the annealing.

1. Introduction

Its single-electron atomic structure and small covalent radius make hydrogen the ideal element to passivate dangling bonds in semiconductors, either crystalline or amorphous, like Si, Ge and SiGe. By such neutralization of the dangling bonds much better electro-optical characteristics are gained. The properties of hydrogenated a-Si, a-Ge and a-SiGe are currently deeply investigated [1–4] because of their promising employment in many devices, like solar cells, IR detectors and because of the many still unsolved issues. Among the latter ones, the behaviour of H is not fully understood and predictable when the above materials are submitted to illumination or thermal treatment [5,6]. A huge literature exists on a-Si and a-SiGe alloys, but not so much for a-Ge and a-Si/a-Ge superlattice nanostructures. The latter ones can be candidate to form the a-SiGe alloy by annealing them so as to intermix Si and Ge and create the alloy [7,8]. In this work we report on the effect of annealing on the properties of hydrogenated a-Si/a-Ge superlattice nanostructures deposited by RF sputtering. Results on annealed hydrogenated single layers of a-Si and a-Ge are also presented as they turned out to be useful to interpret the behaviour of H in the superlattices.

2. Experimental

The hydrogenated a-Si/a-Ge superlattice (SL) nanostructures were deposited by RF sputtering in a conventional high vacuum sputtering apparatus (Leybold Z400), operated at 5×10^{-5} Pa or less. High purity crystalline silicon and germanium targets were used set at 50 mm far from the polished (1 0 0) Si substrate. Sputtering was done with a mixture of high purity argon and hydrogen gases. Growth rate was 6.3 and 13.5 nm/min for a-Si and a-Ge, respectively. The SLs consisted of fifty couples of alternating a-Si and a-Ge layers, 3 nm thick each, yielding a SL thickness of 300 nm. Hydrogenation was achieved by letting H flow into the sputtering chamber during the whole deposition period. H flow rates were 0.4, 0.8, and 1.5 ml/min. The samples were annealed in high purity (99.999%) argon at 350 °C or 400 °C for 1, 4 and 10 h. Single, 40 nm thick, layers of a-Si and a-Ge were also grown, under the same conditions, to measure the H incorporation efficiency.

The samples were analysed by STEM (Scanning Transmission Electron Microscopy) in the HAADF (High Angle Annular Dark Field) mode, ERDA (Elastic Recoil Detection Analysis), AFM (Atomic Force Microscopy) and Infrared (IR) Absorption. For STEM-HAADF in a JEOL 2200 FS machine the SLs were prepared in cross-sectional view by assembling a piece of a sample in a sandwich between 2 Si slabs. The sandwich was then mechanically ground down to 40 μm and finally thinned to electron transparency by Ar ion beam bombardment at 5–3 kV and 3.5 mA. For ERDA the 1.6 MeV $^4He^+$ beam available at the 5 MeV Van de Graaf accelerator of Budapest was applied to measure the H in the samples. The recoiled H signal was collected by an Si detector placed at 10° detecting angle with regard to the beam direction, with the sample tilted 85° to the normal. A 6 μm thick Mylar foil placed in front of the ERDA detector stopped the forward scattered He ions, so that the ERDA spectra for H were almost background-free. Low ion current (~6 nA) was used to avoid beam heating. Evaluation of ERDA spectra was done by RBX program developed by Kótai [9]. A VEECO Dimension 3100 in

* Corresponding author. Tel.: +39 0521 269235; fax: +39 0521 269206.
E-mail address: frigeri@imem.cnr.it (C. Frigeri).

0169-4332/$ – see front matter © 2012 Elsevier B.V. All rights reserved.
http://dx.doi.org/10.1016/j.apsusc.2012.05.030

tapping mode was employed for the AFM analysis. IR absorbance gave information on how H bonds to Si and Ge before and after annealing. An Oriel Cornerstone instrument was used.

3. Results and discussion

The as-sputtered SLs and single layers were amorphous as checked by electron diffraction in the TEM [10]. No area of the crystalline Si substrate was amorphous confirming that the amorphous state was not caused by the ion beam thinning. The samples remained amorphous after annealing [10], as could be expected because the used annealing temperatures were ≤400 °C, i.e. below the crystallization temperature of Ge, which is 450–475 °C [11] or 490 °C [12], and of Si, which is 700–725 °C [11] or 740 °C [12]. The H incorporation in a-Si and a-Ge as a function of the H flow rate was determined by ERDA measurements on the unannealed single layer samples. The ERDA results of this calibration are shown in Fig. 1. H is incorporated more than twice more efficiently in a-Si than in a-Ge. The H content exhibits an asymptotic behaviour at the highest H flow rates reaching a value of ∼17.6 at% and ∼7 at% for a-Si and a-Ge, respectively, at the H flow rate of 1.5 ml/min.

Fig. 2(a) is the STEM-HAADF image of the bottom part of an SL nanostructure on the substrate side. A HAADF image is formed by collecting the incoherently scattered electrons at high angles (Rutherford scattering) [13,14]. Single atoms scatter incoherently and the image intensity is the sum of individual atomic scattering contributions [15]. The HAADF intensity turns out to be proportional to Z^2, with Z the atomic number [13,14,16]. Ge layers appear thus brighter than the Si ones. The layer thickness from Fig. 2(a) averaged over some FWHMs of intensity profiles across the layers turned out to be 2.97 (±6%) nm for both types of layers, in good agreement with expected values.

The unannealed SLs did not show any structural modification upon annealing with an RMS roughness of 0.193 nm. Structural modifications in the shape of blistering was instead observed in the annealed hydrogenated SLs, with the formation of surface bubbles by plastic deformation whose density and size increased with increasing H content, for the same annealing conditions [17]. A typical surface image of an annealed SL is given in Fig. 2(b). Bubble height is on the order of some tens of nm whist the lateral size is on the order of a few μm. Along with such structural surface degradation a change of the H bonding configuration to Si and Ge also occurs as detected by IR absorbance measurements. Fig. 3 illustrates the case of an SL hydrogenated at a flow of 1.5 ml/min and annealed at 400 °C for 1 and 10 h. In the as-deposited, unannealed layer

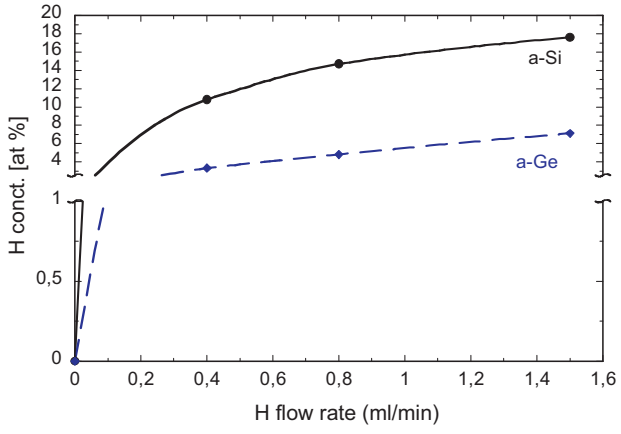

Fig. 1. Calibration curve of the total H concentration incorporated in a-Si (solid black line) and a-Ge (dash blue line) as a function of the H flow rate as determined by ERDA measurements in the single layers. (For interpretation of the references to color in this figure legend, the reader is referred to the web version of the article.)

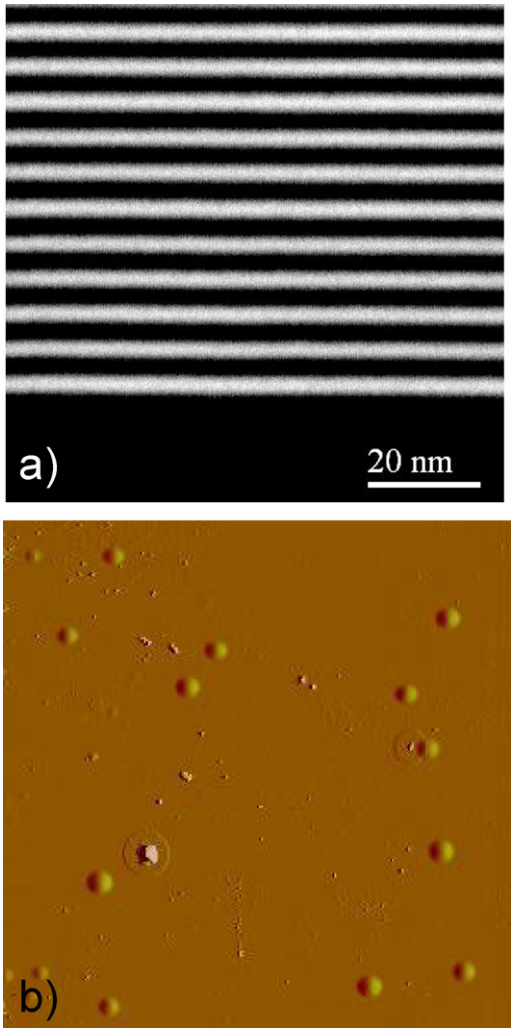

Fig. 2. (a) Typical STEM-HAADF image of the first grown layers of the a-Si/a-Ge SL nanostructures. The bright stripes are the a-Ge layers, while the dark ones are a-Si. The very first grown amorphous layer is Si; it cannot be distinguished from the Si substrate. Interface roughness is partially due to the growth process and partially to pixelating of the digital image (pixel size 0.17 nm). (b) Typical AFM image of blistering in an a-Si/a-Ge SL (H flow rate 1.5 ml/min) annealed at 350 °C for 10 h. Area size 50 μm × 50 μm. Average bubble height and diameter are 80 nm and 2.5 μm, respectively; bubble density 6.7×10^5 cm^{-2}.

(spectrum C1) H is bonded to Ge and Si as monohydride as shown by the peaks at 1880 cm^{-1} and at 2010 cm^{-1}, respectively, which are the fingerprints of such bonds [18–21]. The shape of the Si—H peak indicates that the peak of the Si di-hydride bond, Si—H_2, at about 2140 cm^{-1} could also exist hidden in the tail of the Si—H peak at high wave numbers. The shift with respect to the standard value of 2100 cm^{-1} can be due to the presence of $(Si—H_2)_n$ poly-hydrides [18,19] or to a possible contamination of the hydrides by oxygen [19]. Upon increasing the annealing time the Si—H and Ge—H bonds progressively break until they almost completely disappear for the annealing time of 10 h (spectra C2 and C3 in Fig. 3). The destruction of the Ge—H bonds is already complete after 1 h, i.e. it is much faster than that of the Si—H bonds. H is totally released from Ge already after 1 h annealing. Annealing thus liberates H to the lattice. This suggests that the bubbles are due to local accumulation of free H.

Surface blistering due to bubbles was also observed in the single layers of a-Si and a-Ge. For the highest H content and most severe annealing conditions applied to the single layers (1.5 ml/min, 350 °C, 4 h) it was observed that in the a-Ge layers the bubbles have transformed into craters, i.e. they blew up because of a high

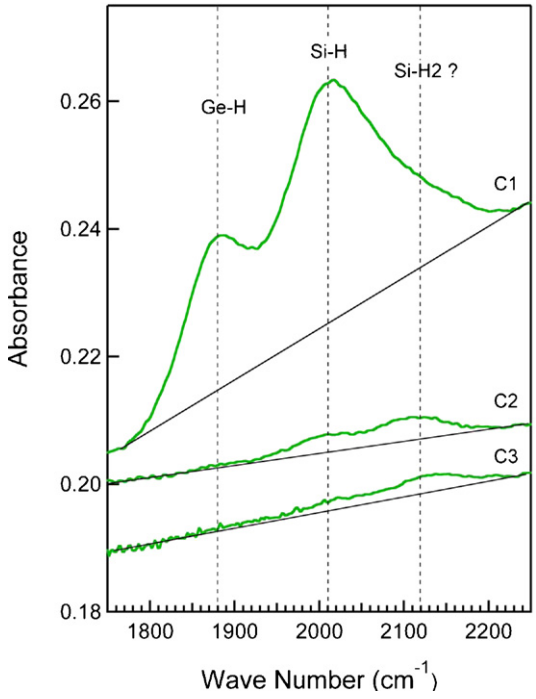

Fig. 3. Typical IR absorbance spectra in the stretching mode range of the wave number for a-Si/a-Ge SLs sputtered under H flow rate of 1.5 ml/min. C1 is the spectrum of the as-deposited layer, C2 the spectrum after annealing at 400 °C for 1 h and C3 the one after annealing at 400 °C for 10 h.

internal gas pressure, while they did not significantly undergo such transformation in a-Si (Fig. 4). This allows to conclude that in a-Ge hydrogen release and formation of H bubbles is more efficient and occurs at an earlier time, with consequent earlier explosion, than in a-Si. For crystalline materials both the yield strength and the ultimate tensile strength are smaller in Ge than in Si [22,23]. Vandeperre et al. have shown that for the yield strength this is also true at temperatures higher than RT, namely in the 350–400 °C range [23]. In the amorphous phase the above strengths should be lower [24]. The anticipated rupture of the Ge layer has thus also to be partially ascribed to the lower mechanical strength of the Ge lattice with respect to Si. Therefore, blistering of the a-Si/a-Ge superlattice nanostructures very likely primarily starts by accumulation of H liberated from the Ge atoms. Nucleation sites for the growth of the bubbles are expected to be nanocavities present in the amorphous phase [18,25].

The ERDA results of Fig. 5 show that the H (at%) remained in the single layers after annealing decreases with respect to the one before to an extent that depends on the annealing time and initial H content, for the same temperature. In a-Ge such decrease is very great (≥∼85 at%) even after 1 h annealing whereas for a-Si that percentage is in the 35–45% range. This is certainly due to the opening of many craters in a-Ge (Fig. 4) through which H largely escapes out. It is expected that in the superlattice samples the H escaped from the Ge layers could remain inside the superlattice as isolated H or gathered into the bubbles because of the presence of the Si layers which have a higher mechanical strength.

The amount of H in the bubbles in the case of Si single layers can be evaluated with the model of lenticular crack proposed by Wan et al. [26]. The much smaller height of the bubbles with respect to their lateral size suggests that they may have a lenticular shape (Figs. 2(b) and 4). The pressure P inside the bubble is then given by [26]

$$P = \frac{16Ehd^3}{3(1-\nu^2)R^4} \quad (1)$$

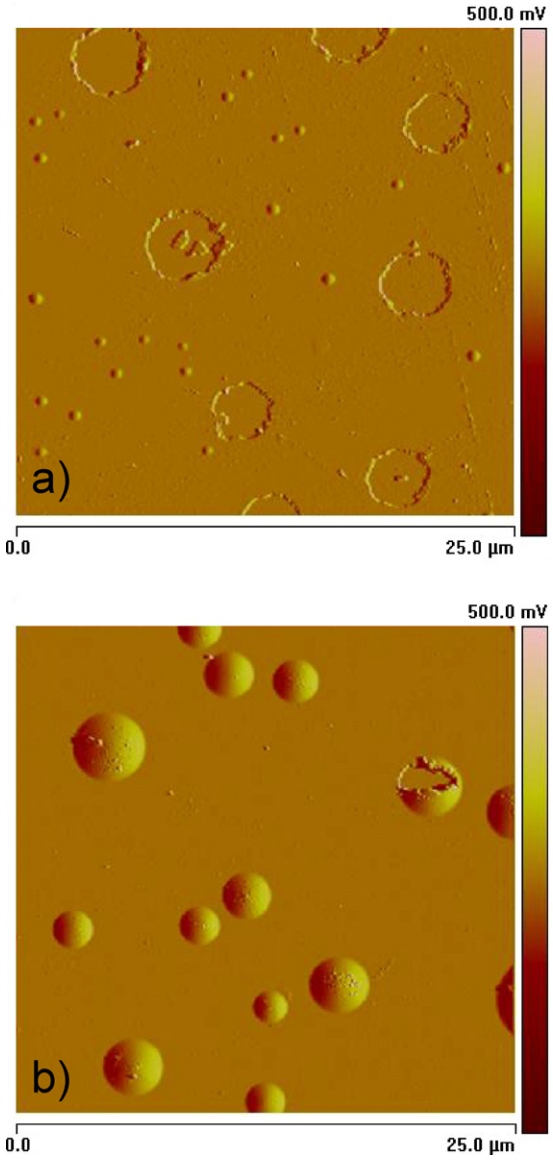

Fig. 4. AFM amplitude image of (a) a-Ge and (b) a-Si single layer after annealing at 350 °C for 4 h. H flow rate 1.5 ml/min. In (a) large craters, i.e. exploded bubbles with escape of H, are predominant. In (b) bumps/blisters (close bubbles with H still inside) are the majority.

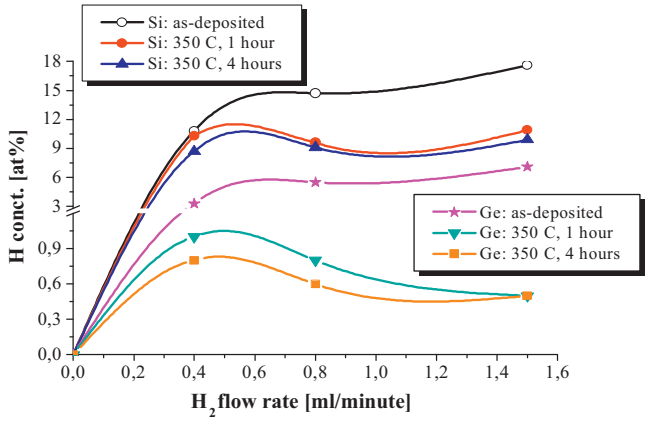

Fig. 5. Hydrogen concentration, as determined by ERDA, as a function of the H flow rate in a-Si and a-Ge single layers before and after annealing at 350 °C for 1 and 4 h. The experimental curve for the as-deposited sample is also shown.

where E is Young's modulus, ν is Poisson's ratio, h is the height of the bubble, R is its radius and d is the thickness of the layer. The relevant data for the Si single layer of Fig. 4(b) are: $E = 130$ GPa, $\nu = 0.28$, $h = 250$ nm, $d = 40$ nm, $R = 0.7$ μm. The latter 3 values are average ones. For E several values have appeared in the literature (see e.g. [27]) ranging roughly from 100 to 200 GPa. Here the values found by Wortman and Evans for E and ν have been chosen [28,29]. With such values the pressure in a bubble is $P = 50$ MPa $= 50$ J/cm^3. The number N of gas molecules in a bubble is given by the gas law,

$$PV = NkT \quad (2)$$

with k the Boltzmann constant, T, the temperature and V, the average bubble volume. Since the craters, i.e. exploded bubbles, are as deep as the whole layer (as deduced from AFM height profiles across craters, not shown here) and do not expand into the substrate, it is assumed that a bubble is a buckling of the whole deposited layer, i.e. that the layer has delaminated in that position. Therefore, for V half the value given by Wan [26], i.e. $V = ½(½\pi hR^2)$, is employed here since a semi-lenticular shape, rather than a full lenticular one, better describes our bubbles. For $T = 350$ °C it is $N = 5.60 \times 10^8$. The density of the bubbles in the sample of Fig. 4(b) is $\rho = 2.24 \times 10^6$ cm^{-2}. The density $\mathcal{N}$ of the H_2 molecules filling all the bubbles in the layer is then $\mathcal{N} = N\rho/d = 3.125 \times 10^{20}$ cm^{-3}.

From Fig. 5 the H present in the Si single layer hydrogenated at the flow of 1.5 ml/min after annealing for 4 h at 350 °C is 9.9 at%. By taking the atomic density of amorphous Si as the one of the crystalline Si (5×10^{22} cm^{-3}) [30] reduced by 1.8% [18], it turns out that the density of the H atoms remained in the a-Si single layer is 4.86×10^{21} cm^{-3}. The total amount $2\mathcal{N}$ of H atoms trapped in the bubbles is therefore 12.9% of the H remained in the layer after annealing. The rest of the unbound H atoms should stay dispersed in the layer as interstitials or inside small bubbles which have not caused blistering and were thus not detected by AFM nor used in the above computation. According to Fig. 3 re-passivation of the Si and Ge dangling bonds should not have occurred.

A rough estimation of the amount of H in the bubbles for the case of an a-Si/a-Ge superlattice could be obtained by the same Wan model [26] applied above. The data for the superlattice of Fig. 2(a) are: $h = 80$ nm, $d = 300$ nm, $R = 1.25$ μm, $\rho = 6.7 \times 10^5$ cm^{-2}. For E the average between its value for Ge ($E = 110$ GPa) [28,29] and Si is used, i.e. $E = 120$ GPa. $\nu = 0.28$ since ν is almost the same for Si and Ge [28,29]. The pressure in a bubble turns out to be 526 MPa with the number of H_2 molecules in a bubble $N = 6.48 \times 10^9$. The total concentration of H atoms in all the bubbles is thus $2\mathcal{N} = 2N\rho/d = 2.90 \times 10^{20}$ cm^{-3} ($d = 300$ nm). The ERDA results of Fig. 5 show that the H remained in the Si and Ge layers after annealing at 350 °C for 4 h is 9.9 and 0.5 at%, respectively. Such data are used for a first approximate estimate of all the H remained in the SL by assuming that the total concentration of the remained H atoms is the sum of the one in the Si layers and the one in the Ge layers. It results that such total concentration is 5.08×10^{21} cm^{-3}. The amount of H atoms in the bubbles is therefore 5.7% of the H remained in the SL after annealing. This lower value with respect to the single layer case may be explained by the lower volume occupied by the bubbles per cubic centimetre of deposited material in the SL (2.37×10^{-3} cm^3/cm^3 in SL vs 5.38×10^{-2} cm^3/cm^3 in single layer), modified (slower) diffusivity of H in the two-phase SL system with respect to the one-phase single layer case, exact location of the H released by Ge (escaped out of the SL through effusion channels or trapped in the Si layers) or other reasons not yet understood.

4. Conclusions

The presented results show that the annealing of hydrogenated a-Si/a-Ge SL nanostructures may have deleterious effects on their structure. Surface bubbles, i.e. blistering, form with a density and size that increase with increasing time and temperature of annealing as well as increasing H content. Annealing also causes de-passivation of the dangling bonds as H is released from its bonds to Si and Ge. Investigations on single layers of Ge and Si suggest that the structural damage, with the formation of H bubbles inside the samples, first starts in the Ge layers because H is released earlier and more efficiently from Ge than from Si and because of the smaller mechanical strength of Ge. The liberated H is partially lost through open craters. ERDA measurements in the single layers, containing the highest amount of H considered here, show that the H remained in the layers is nearly 15% and 55–65% of the incorporated one for Ge and Si, respectively. The total amount of H atoms trapped in the bubbles is around 13% of those remained in the a-Si single layer. No estimation for Ge was possible because the surface bubble density could not be reliably measured by AFM. For the SLs an approximate evaluation suggests that the H atoms trapped in the bubbles are 5.7% of those remained inside. However, modelling and calculation need improvement. A key parameter is the shape, hence volume of the bubbles. The assumption made in this work is that they have a semi-lenticular shape. Alternatively a semi-ellipsoidal shape could be assumed. In such a case the volume of a bubble ($1/2(4/3\pi hR^2)$), hence the density of the atoms trapped in the bubbles, increases by a factor 2.66. The bubble volume issue is more critical in the case of the SLs as the bubble shape might be more complex than in the single layers since it might be irregular because of the different elastic properties of Si and Ge and depending on whether the bubble fully extends down to the substrate surface or not. A better estimation of the shape could be provided by future AFM observations in cross-sectional view. Whatever is the shape of the bubbles their H content will always be somewhat underestimated if some bubbles do not produce blistering and cannot be detected by AFM.

As regard the formation of the a-SiGe alloy from the studied a-Si/a-Ge SLs previous findings have shown that Si and Ge interdiffusion actually occurs across the interfaces [17,31–33]. However, complete intermixing so as to form a homogeneous SiGe alloy in place of the SL has not been achieved as yet. The optimum compromise among annealing conditions, H content and layer thickness has to be looked for.

Acknowledgements

Work supported by the Scientific Cooperation Agreement between CNR (Italy) and MTA (Hungary) under the contract MTA 1102, as well as by OTKA Grant Nos. K-67969, CK-80126, and TAMOP 4.2.1./B-09/1/KONV-2010-0007 project (implemented through the New Hungary Development Plan cofinanced by the European Social Fund, and the European Regional Development Fund). Z. Erdélyi is a grantee of the 'Bolyai János' scholarship. National Office for Research and Technology (Hungary, NKTH) is also acknowledged for the support via Grant No. TFSOLAR2.

References

[1] Y. Qin, T. Feng, Z. Li, Z. Sun, Applied Surface Science 257 (2011) 7993–7996.
[2] J. Müllerová, L. Prusáková, M. Netrvalová, V. Vavrunková, P. Sutta, Applied Surface Science 256 (2010) 5667–5671.
[3] Y. Hamakawa, Journal of Non-Crystalline Solids 352 (2006) 863–867.
[4] K.W. Jobson, J.-P.R. Wells, R.E.I. Schropp, D.A. Carder, P.J. Philips, J.I. Dijkhuis, Physical Review B 73 (2006) 155202.
[5] J.D. Cohen, Solar Energy Materials and Solar Cells 78 (2003) 399–424.
[6] P. Agarwal, S.C. Agarwal, Philosophical Magazine B 80 (2000) 1327–1346.
[7] T. Sameshima, H. Watanabe, H. Kanno, T. Sadoh, M. Miyao, Thin Solid Films 487 (2005) 67–71.
[8] M.S. Abo Ghazala, Physica B 293 (2000) 132–136.
[9] E. Kótai, in: J.L. Duggan, I.L. Morgan (Eds.), Proc. of 14th Int. Conf. on Appl. Accelerators in Res. Ind., Denton, USA, 1996, AIP Press, New York, 1997, p. 631.
[10] C. Frigeri, M. Serényi, A. Csik, Z. Erdélyi, D.L. Beke, L. Nasi, Journal of Materials Science – Materials in Electronics 19 (2008) S289–S293.

[11] Zs. Czigány, G. Radnóczi, K. Järrendahl, J.-E. Sundgren, Journal of Materials Research 12 (1997) 2255–2261.
[12] J.C.C. Fan, C.H. Anderson, Journal of Applied Physics 52 (1981) 4003–4006.
[13] S.J. Pennycook, S.D. Berger, R.J. Culbertson, Journal of Microscopy 144 (1986) 229–249.
[14] S.J. Pennycook, D.E. Jesson, Ultramicroscopy 37 (1991) 14–38.
[15] D.B. Williams, C.B. Carter, Transmission Electron Microscopy, vol. 3, Springer, New York, 1996 (Chapter 22).
[16] T. Walther, Journal of Microscopy 221 (2006) 137–144.
[17] C. Frigeri, L. Nasi, M. Serényi, A. Csik, Z. Erdélyi, D.L. Beke, Superlattices and Microstructures 45 (2009) 475–481.
[18] S. Acco, D.L. Williamson, P.A. Stolk, F.W. Saris, M.J. van den Boogaard, W.C. Sinke, W.F. van der Weg, S. Roorda, P.C. Zalm, Physical Review B 53 (1996) 4415–4427.
[19] M. Daouahi, K. Zellama, H. Bouchriha, P. Elkaïm, European Physical Journal-Applied Physics 10 (2000) 185–191.
[20] C. Manfredotti, F. Fizzotti, M. Pastorino, P. Polesello, E. Vittone, Physical Review B 50 (1994) 18046–18053.
[21] R.J. Soukup, N.J. Ianno, S.A. Darveau, C.L. Exstrom, Solar Energy Materials and Solar Cells 87 (2005) 87–98.
[22] A.L. Ruoff, Journal of Applied Physics 49 (1978) 197–200.
[23] L.J. Vandeperre, F. Giuliani, S.J. Lloyd, W.J. Clegg, Acta Materialia 55 (2007) 6307–6315.
[24] X. Zhu, J.S. Williams, D.J. Llewellyn, J.C. McCallum, Applied Physics Letters 74 (1999) 2313–2315.
[25] W. Beyer, Solar Energy Materials and Solar Cells 78 (2003) 235–267.
[26] K.-T. Wan, R.G. Horn, S. Courmont, B.R. Lawn, Journal of Materials Research 8 (1993) 1126–1136.
[27] http://www.memsnet.org/material/siliconsibulk/.
[28] J.J. Wortman, R.A. Evans, Journal of Applied Physics 36 (1965) 153–156.
[29] http://www.ioffe.ru/SVA/NSM/Semicond/Si/mechanic.html.
[30] A.S. Groove, Physics and Technology of Semiconductor Devices, J. Wiley, New York, 1967 (Chapter 4).
[31] A. Csik, G.A. Langer, D.L. Beke, Z. Erdélyi, M. Menyhard, A. Sulyok, Journal of Applied Physics 89 (2001) 804–806.
[32] A. Csik, D.L. Beke, G.A. Langer, Z. Erdélyi, L. Daroczi, K. Kapta, M. Kis-Varga, Vacuum 61 (2001) 297–301.
[33] A. Simon, A. Csik, F. Paszti, A.Z. Kiss, D.L. Beke, L. Daroczi, Z. Erdélyi, G.A. Langer, Nuclear Instruments and Methods in Physics Research B 161 (2000) 471–475.